Lagrangian Statistics of Navier-Stokes- and MHD-Turbulence

Holger Homann and Rainer Grauer*
Theoretische Physik I, Ruhr-Universität Bochum, Germany

Angela Busse and Wolf-Christian Müller
MPI for Plasma Physics, Garching, Germany
(Dated: May 31, 2007)

We report on a comparison of high-resolution numerical simulations of Lagrangian particles advected by incompressible turbulent hydro- and magnetohydrodynamic (MHD) flows. Numerical simulations were performed with up to 1024^3 collocation points and 10 million particles in the Navier-Stokes case and 512^3 collocation points and 1 million particles in the MHD case. In the hydrodynamics case our findings compare with recent experiments from Mordant et al. [1] and Xu et al. [2]. They differ from the simulations of Biferale et al. [3] due to differences of the ranges choosen for evaluating the structure functions. In Navier-Stokes turbulence intermittency is stronger than predicted by a multifractal approach of [3] whereas in MHD turbulence the predictions from the multifractal approach are more intermittent than observed in our simulations. In addition, our simulations reveal that Lagrangian Navier-Stokes turbulence is more intermittent than MHD turbulence, whereas the situation is reversed in the Eulerian case. Those findings can not consistently be described by the multifractal modeling. The crucial point is that the geometry of the dissipative structures have different implications for Lagrangian and Eulerian intermittency. Application of the multifractal approach for the modeling of the acceleration PDFs works well for the Navier-Stokes case but in the MHD case just the tails are well described.

PACS numbers: 47.27.-i, 47.10.+g,52.30Cv, 52.35.Ra, 52.65.Kj

Introduction Lagrangian statistics of turbulent flows has undergone a rapid development in the last 6 years due to enormous progress in experimental techniques measuring particle trajectories. Particle tracking velocimetry has been used for moderate Reynolds numbers by [4]. However, the techniques developed in Cornell [5–7] and Lyon [1, 8] allowed the measurements of probability density functions (PDFs) of velocity increments which triggered a renewed interest in the theoretical understanding of Lagrangian statistics. A very promising approach based on a Markovian closure was recently introduced in [9]. This approach is not readily applicable to magnetohydrodynamic (MHD) turbulence, since the distribution function depends not only on velocity, space and initial condition but in addition on the Jacobian. Although work in this direction is in progress, we compare our simulations to a phenomenological model of Lagrangian statistics in Navier-Stokes turbulence introduced by Biferale et al. [3]. Our findings show increased intermittency in Navier-Stokes flows, such that the structure functions agree with recent experimental data from the two experimental groups [1, 2]. On the other hand, our MHD simulations are less intermittent than the predictions from a multifractal model.

Numerical Methods The Lagrangian particle trajectories were obtained by two slightly different parallel spectral codes (Garching and Bochum) based on the spectral code used in [10]. The velocity and magnetic field was evaluated at the particle positions using either trilinear or tricubic interpolation. Contrary to the simulations of [3], we found that tricubic interpolation captures especially trajectories with high acceleration more precise than linear interpolation, a conclusion which was drawn already 20 years ago (see [11] and the discussion therein). However, the effect of the slightly different trajectories has only a minor effect on the tails of the acceleration PDFs with the tendency that the PDF calculated with tricubic interpolation is slightly more intermittent than the corresponding one calculated with trilinear interpolation. The simulations presented here use a tricubic interpolation for obtaining the velocities at the particle positions.

Navier-Stokes turbulence We performed a set of simulations for the Navier-Stokes-equations with two resolutions, 512^3 and 1024^3 collocation points and 1 million and 10 million particles, respectively, in order to obtain reliable statistical results within a few large eddy-turnover times.

Parameters of all simulations (Navier-Stokes and MHD) are summarized in Table I. Here we used the same conventions as described in [12]. To get to a stationary turbulent state, we started with randomly distributed Fourier-modes without driving. After the turbulence has been fully developed, the low mode number modes were kept constant. Particles with initially homogeneous random positions were injected when a stationary state was reached. For the simulation with 1024^3 collocation points, we started from the stationary turbulent state with 512^3 collocation points. The relaxation to a new stationary state took about one large-eddy turnover

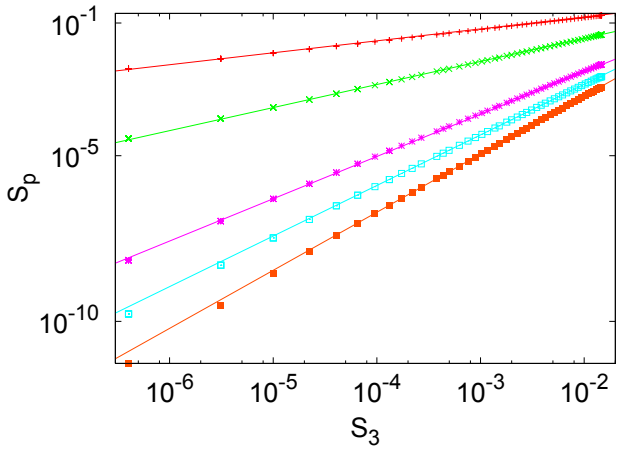

FIG. 1: Eulerian structure functions of order p=1,2,4,5,6 (top to bottom)

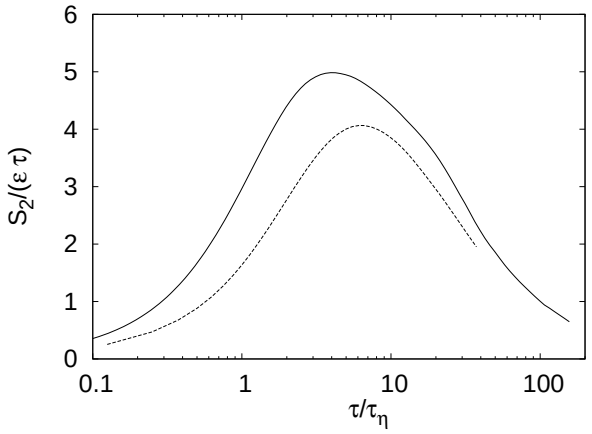

FIG. 2: 2nd order structure function normalized to $\epsilon\tau$ for Run1 (solid line) and Run4 (dashed line)

time. After this period, the particles were injected.

The choice of the parameters for Run1, Run4 and Run5 and therefore the resulting Taylor microscale Reynolds number was motivated by the standard procedure to choose the dissipation length l_d smaller than the grid spacing [13]. However, recent investigations of how dissipative structures like shocks, tubes and sheets enter the dissipation range [14–16] suggest a more conservative choice which was realized in Run2 and Run3.

The exponents of the longitudinal Eulerian structure functions $S_p =< |\mathbf{u}(\mathbf{x}+\mathbf{l}) - \mathbf{u}(\mathbf{x})|^p >$, angular brackets denoting spatial averaging, can be described by the She-Lévêque formula [17, 18] for the simulations Run1 - Run3. The structure functions using extended self similarity (ESS) [19] together with straight lines illustrating the fitted slopes are shown in Figure 1 for data obtained from Run3. The values of the corresponding exponents are summarized in Table II. These Eulerian statistics serve just as a test to check the numerics.
The determination of the Lagrangian structure functions $S_p =< |\mathbf{u}(t+\tau) - \mathbf{u}(t)|^p >$, angular brackets denoting temporal averaging, turned out to be much more difficult. Figure 2 shows a typical plot of the second order Lagrangian structure function normalized to $\epsilon\tau$. It is clear that no scaling range is present as already observed in the experiments [1, 2] and simulation [3, 20]. Therefore, in order to obtain scaling exponents one has to rely on the assumption of extended self similarity. Figure 3 shows an evaluation of the Lagrangian structure functions assuming ESS. In Table III we present the relative exponents ζ_p/ζ_2 for our simulations. In addition, this table contains also exponents collected from the experiments [1, 2] and other numerical simulations [1, 3].

First, we observe that the simulations Run1 - Run3 all give exponents which agree within the error bars. Thus, a possible dependence of the exponents on the Reynolds number or the choice of a stricter criterion for the numer-

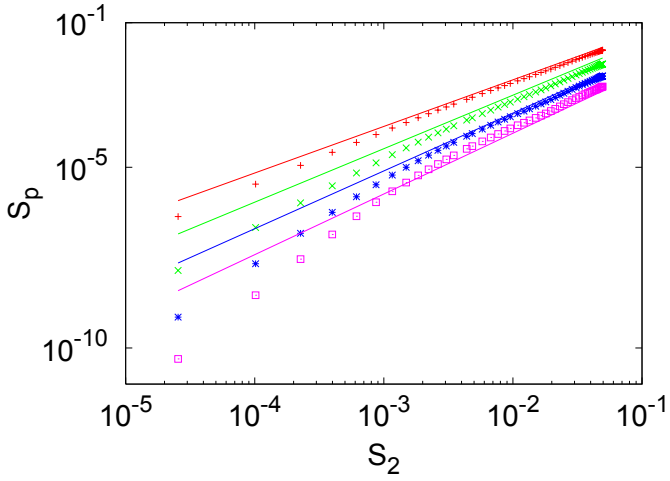

FIG. 3: Lagrangian structure functions from Run3 of order p=3-6 (top to bottom)

ical resolution could not be detected given the relative large error bars. In addition, the exponents fit quite well to the present experiments [1, 2] but are clearly different from the exponents obtained by [3]. The reason for this is not the different interpolation for particle velocities (trilinear in [3], tricubic here). We repeated a simulation with the parameters of Run2 but using trilinear interpolation and got the same scaling as with tricubic interpolation. We explain this discrepancy similar as in [2] by observing that the evaluation of the structure functions was performed systematically using larger values of τ compared to us. We have have chosen the inertial range from Figure 2 by the requirement that the function stays above ninety percent of its maximum value. This leads to an inertial range of $2 \leq \tau \leq 7$.We are able to reproduce the exponents of [3] if we choose a minimal value of τ of about eight. Larger values of τ result in a more Gaussian behavior and explains why the exponents of [3]

R_λ	u_0	ϵ_k	ϵ_m	$\nu=\eta$	dx	l_d	τ_d	L	T_L	T/T_L	N^3	N_p	
190	0.82	0.23	-	$8\cdot10^{-4}$	$12.27\cdot10^{-3}$	$6.9\cdot10^{-3}$	$5.9\cdot10^{-2}$	2.4	2.9	10.3	512^3	$1.18\cdot10^6$	Run1
122	0.16	$2.1\cdot10^{-3}$	-	$3\cdot10^{-4}$	$12.27\cdot10^{-3}$	$1.1\cdot10^{-2}$	$3.7\cdot10^{-1}$	1.9	12	5	512^3	$1\cdot10^6$	Run2
178	0.16	$2\cdot10^{-3}$	-	$1.5\cdot10^{-4}$	$6.14\cdot10^{-3}$	$6.4\cdot10^{-3}$	$2.8\cdot10^{-1}$	2	11	2	1024^3	$10\cdot10^6$	Run3
187	0.48	0.1	0.15	$5\cdot10^{-4}$	$12.27\cdot10^{-3}$	$5.9\cdot10^{-3}$	$7.1\cdot10^{-2}$	2.4	5	4.7	512^3	$1.18\cdot10^6$	Run4
234	0.22	$1\cdot10^{-2}$	$1.5\cdot10^{-2}$	$1.5\cdot10^{-3}$	$12.27\cdot10^{-3}$	$4.3\cdot10^{-3}$	$1.2\cdot10^{-1}$	2.5	6.3	1.8	512^3	$1\cdot10^6$	Run5

TABLE I: Parameters of the numerical simulations. R_λ: Taylor microscale Reynolds number $\sqrt{15u_0L/\nu}$, $u_0=\sqrt{2/3E_k}$, E_k: kinetic energy, E_m: magnetic energy, $E=E_k+E_m$, ϵ_k: kinetic energy dissipation rate, ϵ_m: magnetic energy dissipation rate, $\epsilon=\epsilon_k+\epsilon_m$, ν: viscosity, η: resistivity, l_d: dissipation lengthscale $(\nu^3/\epsilon_k)^{1/4}$, τ_d: Kolmogorov time scale $(\nu/\epsilon_k)^{1/2}$, $L=(2/3E)^{3/2}/\epsilon$: integral scale, $T_L=L/u_0$: large-eddy turnover time, T: total integration time, N^3: number of collocation points, N_p: number of particles, Navier-Stokes simulations: Run1-Run3, MHD simulations: Run4, Run5

are less intermittent.

We also applied the multifractal model to the acceleration statistics obtained from the simulations. We shortly review the approach of [3]. One starts with a suitable description for the Eulerian structure functions, e.g. the She-Lévêque model [17] and performs a Legendre transformation to obtain the singularity spectrum. In order to translate Eulerian to Lagrangian increments, one assumes a Kolmogorov like relation $\delta_\tau v\sim\delta_l u$ where temporal and spatial increments are related by $\tau_l\sim l/\delta_l u$. The resulting expression for the Lagrangian structure functions,

$$S_p(\tau)\sim\langle v_0^p\rangle\int_{h\in I}dh\,\left(\frac{\tau}{T_L}\right)^{\frac{hp+3-D(h)}{1-h}}, \qquad (1)$$

is evaluated by a saddle point integration. To obtain the acceleration PDF, first the acceleration is defined as $a=\frac{\delta_{\tau_\eta}v}{\tau_\eta}$ where $\tau_\eta=\tau_\eta(h,u_0)$ is the Kolmogorov time scale which is itself a multifractal quantity depending on the large scale velocity field u_0. Assuming a Gaussian statistics of u_0 and integrating over the possible scaling factors h results in an explicit expression for the acceleration PDF (see [3] for details)

$$P(a)\sim\int_{h_{\min}}^{h_{\max}}dh\quad\tilde{a}^{((h-5+D(h))/3)}R_\lambda^{y(h)}\exp\left(-\frac{1}{2}\tilde{a}^{2(1+h)/3}R_\lambda^{z(h)}\right)$$

order	She-Lévêque	Run3
1	0.364	0.36 ± 0.0027
2	0.696	0.696 ± 0.0027
3	1	1
4	1.279	1.276 ± 0.0053
5	1.538	1.526 ± 0.013
6	1.778	1.752 ± 0.024
7	2.001	2.028 ± 0.088
8	2.211	2.204 ± 0.087

TABLE II: Eulerian structure functions obtained using ESS with $\zeta_3=1$.

with $\tilde{a}=a/\sigma_a$, $\sigma_a=\langle a^2\rangle^{1/2}$, $y(h)=\chi(h-5+D(h))/6+2(2D(h)+2h-7)/3$ and $z(h)=\chi(1+h)/3+4(2h-1)/3$. A comparison of the multifractal prediction to the numerically obtained acceleration PDFs is shown in Figure 4. Although there is an excellent agreement between prediction and simulation, one has to keep in mind that the multifractal prediction contains three parameters. The first parameter is hidden in the relation $\langle a^2\rangle\propto R_\lambda^\chi$ when normalizing the width of the PDF. However, this parameter can be determined from one simulation and should then be kept fixed for other Reynolds numbers. In the She-Lévêque model, the value of $h_{\min}$ is given by $h_{\min}=1/9$. If one uses this value, it is not possible to get good agreement with the measured shape of the PDF. Therefore, as in [3], we use $h_{\min}$ as a free parameter. The last is a free amplitude in the normalization. In order to get such an excellent agreement in Figure 4, we had to choose $h_{\min}=0.175$ for Run2 and $h_{\min}=0.16$ for Run3. The dependence on $h_{\max}$ is negligible.

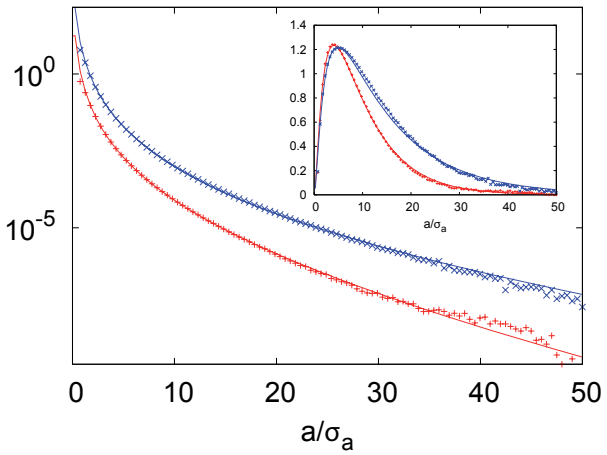

FIG. 4: Acceleration PDFs for runs Run2(+) and Run3(x) including the PDFs using the multifractal approach for the Navier-Stokes simulations. The inset shows the PDF multiplied by $(a/\sigma)^4$.

order	Run1	Run2	Run3	MF-NS	Simulation [3]	Experiment [1]	Simulation [1]	Experiment [2]
R_λ	190	122	178		284	1000	140	815
1	0.58 ± 0.006	0.57 ± 0.007	0.57 ± 0.005	0.55	-	0.56 ± 0.01	0.56 ± 0.02	0.58 ± 0.12
2	1	1	1	1	1	1	1	1
3	1.28 ± 0.020	1.29 ± 0.025	1.30 ± 0.016	1.38	-	1.34 ± 0.02	1.3 ± 0.04	1.28 ± 0.30
4	1.46 ± 0.06	1.48 ± 0.066	1.51 ± 0.041	1.71	1.7 ± 0.05	1.58 ± 0.06	1.5 ± 0.09	1.47 ± 0.38
5	1.58 ± 0.12	1.60 ± 0.12	1.65 ± 0.075	2.00	2.0 ± 0.05	1.76 ± 0.1	1.61 ± 0.13	1.59 ± 0.46
6	1.67 ± 0.19	1.68 ± 0.18	1.76 ± 0.11	2.26	2.2 ± 0.07	1.9 ± 0.2	1.69 ± 0.2	1.66 ± 0.53

TABLE III: Relative ESS-exponents calculated with respect to the structure function of order 2. MF-NS denotes the Multi-Fractal approach for Navier-Stokes.

MHD turbulence The parameters for the MHD simulations are summarized in Table I (Run4, Run5). Both runs were performed with negligible magnetic and cross helicity. ESS plots of the Lagrangian velocity structure

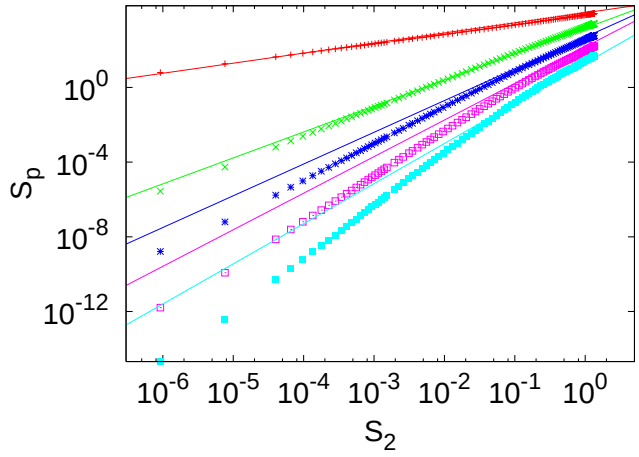

FIG. 5: Lagrangian structure functions from Run4 of order 1,3,4,5,6 (top to bottom)

functions are shown in Figure 5. They show a similar curved shape although no trapping in vortex tubes appears in MHD turbulence (see also Biferale et al. [21]).

The exponents for the Lagrangian velocity structure functions are given in Table IV. Also shown is the prediction by a multifractal model, which was obtained using the same steps as described above, but starting with a She-Lévêque like formula suitable for incompressible MHD-turbulence [10, 22],

$$\zeta_L^{\mathrm{MHD}}(p) = \frac{p}{9} + 1 - \left(\frac{1}{3}\right)^{p/3} . \qquad (2)$$

Although this formula is strictly valid only for the structure functions of the Elsässer variables $\mathbf{z}^{\pm} = \mathbf{u} \pm \mathbf{B}$, we assume a cascade in the kinetic energy so that this formula can also be applied to the structure functions of velocity. The resulting multifractal model shows now an increased degree of intermittency compared to the numerical simulations (Run4, Run5). On the first sight this is astonishing since this is just the opposite behavior as in the Navier-Stokes case. To summarize, we have the following situation that in the Eulerian description, MHD turbulence is more intermittent than Navier-Stokes turbulence whereas the situation is reversed in the Lagrangian picture. This finding is also not compatible with the multifractal ansatz. The multifractal ansatz possesses a certain *monotonicity* property. This means that if for two different sets of structure function exponents, one is more intermittent than the other in the Eulerian picture, than this one is also more intermittent in the Lagrangian turbulence. To see this, it is sufficient to look at high values p of the order of the structure functions. One observes that the value of h^* where the infimum of

$$hp + 3 - D(h)$$

is assumed goes to $h_{\min}$ for high values of p. Thus the asymptotic behavior reads

$$\zeta_p = h_{\min} p + 3 - D(h_{\min}) \quad , \quad p \gg 1 .$$

For the saddle point evaluation of the Lagrangian structure functions (see eqn. 1) one has to find the infimum of

$$\frac{hp + 3 - D(h)}{1 - h}$$

so that the asymptotic behavior is given by

$$\zeta_p = \frac{h_{\min} p + 3 - D(h_{\min})}{1 - h_{\min}} \quad , \quad p \gg 1 .$$

Since both in Navier-Stokes and MHD the value of $h_{\min} = 1/9$ is identical, the degree of intermittency is determined by $D(h_{\min})$. This is both valid for the Eulerian as well as for the Lagrangian model which guarantees the *monotonicity* property.

Our conclusion from this numerical observation is that the geometry of the most singular structures (vortex tubes and current sheets) is not the right quantity to determine the degree of Lagrangian intermittency, but it is more important to look at the tracer dynamics. In Figure 6 particle trajectories with high acceleration near singular structures are shown. Here the isosurfaces belong to a fixed point in time. Important is that in the

order	Run4	Run5	MF-MHD
R_λ	187	270	
1	0.527 ± 0.004	0.526 ± 0.002	0.63
2	1	1	1
3	1.412 ± 0.013	1.407 ± 0.014	1.26
4	1.76 ± 0.04	1.73 ± 0.06	1.47
5	2.06 ± 0.08	1.96 ± 0.14	1.65
6	2.24 ± 0.24	2.11 ± 0.25	1.81

TABLE IV: Relative ESS-exponents calculated with respect to the structure function of order 2.

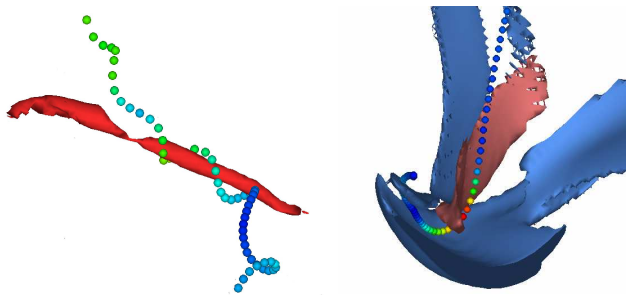

FIG. 6: Trajectories with high acceleration in NS (left) and MHD (right, blue denotes current density and red vorticity).

MHD case the trajectories near the sheet structures are smooth. Thus contrary to the Eulerian point of view where the sheets are responsible for producing intermittency, they do not contribute significantly to Lagrangian intermittency. Large changes with high acceleration occur at the ends of the sheet structures. Thus a naive translation of Eulerian to Lagrangian structures is not possible. A more detailed investigation of the relation between Lagrangian intermittency and the small-scale structure of dissipation will be presented elsewhere. Using the multifractal approach we also compared the PDFs of velocity and magnetic field increments of the order of the Kolmogorov time with the multifractal prediction which is depicted in Figure 7, again assuming the validity of (2) for the velocity and magnetic field. Here, we have chosen $h_{\min} = 0.16$ to obtain the best agreement between the model and prediction. The agreement is not as perfect as in the Navier-Stokes case. Here, only the exponential tail could be well described by the multifractal model.

Conclusions and open questions The presented Navier-Stokes simulations show good agreement with recent experiments but deviate from predictions of a multifractal model. An observation which also could not be described by multifractal modeling is that Lagrangian Navier-Stokes intermittency is stronger than in the MHD case whereas the situation is reversed for Eulerian statistics. The present situation is depicted in Figure 8. It shows that the multifractal prediction for Lagrangian

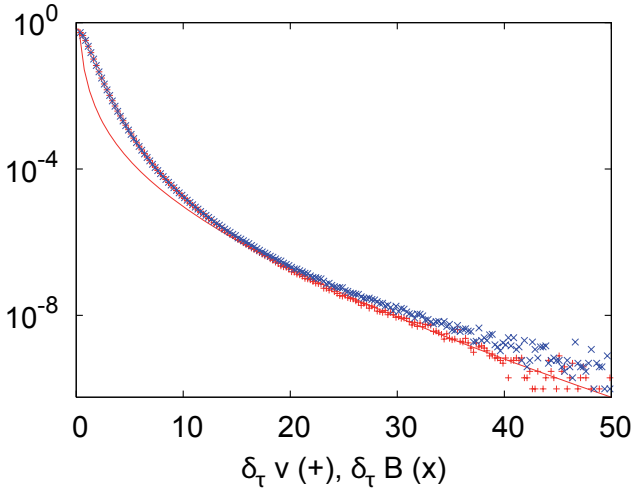

FIG. 7: Comparison of PDFs of velocity(+) and magnetic field(x) increments for small τ: magnetic field increment are broader. The continuous line corresponds to the multifractal approach.

Navier-Stokes turbulence fits well to the simulations of Lagrangian MHD turbulence and vice versa. This again shows that it is not easily possible to relate the geometry of the most dissipative structures to the strong acceleration events.

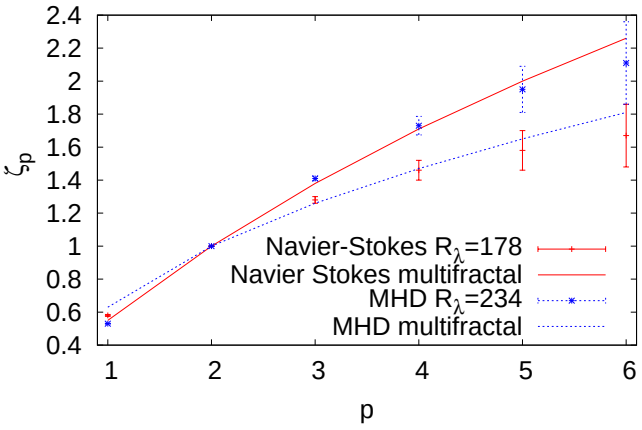

FIG. 8: Comparison of measured scaling exponents to the multifractal prediction

A second and related critical issue in the Lagrangian treatment is the validity of the Kolmogorov like relation $l \sim \tau u_l$ which connects Eulerian and Lagrangian quantities. At least in the neighborhood of strongly dissipating structures (tubes and sheets) this relation has to be altered to $l \sim \tau u_0$ where u_0 is the mean flow produced by the vortex. A similar reasoning was given in [23] to calculate the basic mechanism for obtaining exponential tails in the PDF of velocity increments.

The partial success of the PDF modeling with the multifractal ansatz is mainly attributed to the freedom of

choosing three free parameters: i) one parameter hidden in the normalization of the Reynolds number, ii) the value of $h_{\min}$ and finally iii) the amplitude. If one fixes $h_{\min}$ to the She-Lévêque value $h_{\min} = 1/9$ then this modeling is not able to reproduce the shape of the PDF.

Thus a deeper understanding of the connection between the geometry of dissipative structures and high acceleration events is necessary to correctly model Lagrangian intermittency.

Acknowledgments.— Access to the JUMP multiprocessor computer at the FZ Jülich was made available through project HB022. Part of the computations were performed on an Linux-Opteron cluster supported by HBFG-108-291. A.B. and WC.M. would like to thank the staff at RZG, Garching and LRZ, Munich for competent and friendly assistance. The work of H.H. and R.G. benefitted from support through SFB 591 of the Deutsche Forschungsgesellschaft.

* Electronic address: grauer@tp1.rub.de

[1] N. Mordant, E. Lévêque, and J.-F. Pinton, New Journ. Phys. **6**, 116 (2004).
[2] H. Xu, M. Bourgoin, N. Ouellette, and E. Bodenschatz, preprint (2005).
[3] L. Biferale, G. Bofetta, A. Celani, B.J. Devinish, A. Lanotte, and F. Toschi, Phys. Rev. Lett. **93**, 064502 (2004).
[4] S. Ott and J. Mann, J. Fluid Mech. **422**, 207 (2000).
[5] A. La Porta, G. Voth, F. Moisy, and E. Bodenschatz, Phys. Fluids **12**, 1485 (2000).
[6] A. La Porta, G. Voth, A.M. Crawford, J. Alexander, and E. Bodenschatz, Nature **409**, 1017 (2001).
[7] G. Voth, A. La Porta, A.M. Crawford, J. Alexander, and E. Bodenschatz, Rev. Sci. Instr. **12**, 4348 (2001).
[8] N. Mordant, P. Metz, O. Michel, and J.-F. Pinton, Phys. Rev. Lett **87**, 214501 (2001).
[9] R. Friedrich, Phys. Rev. Lett. **90**, 084501 (2003).
[10] W.C. Müller and D. Biskamp, Phys. Rev. Lett. **84**, 475 (2000).
[11] P.K. Yeung, Annu. Rev. Fluid Mech. **34**, 115 (2002).
[12] U. Frisch, *Turbulence. The Legacy of A.N. Kolmogorov* (Cambridge University Press, Cambridge, England, 1995).
[13] P.K. Yeung and S.B. Pope, J. Fluid Mech. **207**, 531 (1989).
[14] M. Lässig, Phys. Rev. Lett. **84**, 2618 (2000).
[15] V. Yakhot and K.R. Sreenivasan, J. Stat. Phys. **121**, 825 (2005).
[16] J. Schumacher, K. R. Sreenivasan und V. Yakhot, in preparation (2006).
[17] Z.-S. She and E. Lévêque, Phys. Rev. Lett. **72**, 336 (1994).
[18] B. Dubrulle, Phys. Rev. Lett. **73**, 959 (1994).
[19] R. Benzi, S. Ciliberto, R. Tripiccione, C. Baudet, F. Massaioli and S. Succi, Phys. Rev. E **48**, R29 (1993).
[20] P. K. Yeung and M. S. Borgas, J. Fluid Mech. **503**, 93 (2004).
[21] L. Biferale, G. Boffetta, A. Celani, A. Lanotte and F. Toschi, Phys. Fluids **17**, 021701 (2005) .
[22] T.S. Horbury and A. Balogh, Nonlin. Proc. Geophys. **4**, 185 (1997).
[23] Y. Li and C. Meneveau, Phys. Rev. Lett. **95**, 164502 (2005).